Applied Numerical Modeling in Geomechanics – 2020 – Billaux, Hazzard, Nelson & Schöpfer (eds.) Paper: 11-05
©2020 Itasca International, Inc., Minneapolis, ISBN 978-0-9767577-5-7

Integrating laser scanning with Discrete Element Modeling for improving safety in underground stone mines

Juan J. Monslave[1], Aman Soni[1], Jim Hazzard[2] & Nino Ripepi[1]
[1] *Department of Mining and Minerals Engineering, Virginia Tech, Blacksburg, VA, USA*
[2] *Itasca Consulting Group, Inc., Minneapolis, MN, USA*

1 INTRODUCTION

According to the Mine Health and Safety Administration (MSHA), between 2006 and 2016 the underground stone mining industry had the highest fatality rate in 4 out of 10 years, compared to any other type of mining in the United States. Additionally, the National Institute for Occupational Safety and Health (NIOSH) stated that structurally controlled instability is a predominant failure mechanism in underground limestone mines (Esterhuizen et al. 2011). This failure mode has been widely described in rock engineering literature and it occurs when fractures present in a rock mass intercept each other, forming rock blocks that displace inside the tunnel as the excavation takes place, posing a significant hazard for miners (Goodman 1989, Brady & Brown 1985, Goodman & Shi 1985). Conventional design guidelines for underground stone mines proposed by NIOSH do not take into account structurally controlled failure. Furthermore, these guidelines are only applicable to room and pillar mines in flat-lying bedded formations located in the eastern and Midwestern United States (Esterhuizen et al. 2011). Due to this, it is necessary to consider a more general design methodology that can be implemented in any mine considering site specific conditions to complement already existing design methods.

This work was developed in an underground limestone mine evidencing a structurally controlled failure mechanism. According to field observation and the risk/Hazard Assessment Chart proposed by Martin et al. (2003), the main cause of instability in this mine is due to gravity-induced structurally controlled block movement, considering a Uniaxial compressive strength of 160 MPa for the rock, an average GSI of 75, and a maximum vertical stress close to 20 MPa at the deepest point in the mine. This operation extracts a 30 m thick and 30° dipping limestone body with a room and pillar mining method with eventual stoping and does not meet the requirements to be designed with NIOSH design guidelines.

In recent years, Terrestrial laser scanning (TLS) has been used to map and characterize fractures present in a rock mass. TLS is a technology that can generate a three-dimensional multimillion point cloud of a scanned area. Moreover, advances in computing power throughout the past years have allowed numerical modeling software such as *3DEC* (Itasca 2016) to represent more realistically the behavior of fractured rock masses. *3DEC* is Discrete Element Modeling software that can simulate the response of a discrete body under either a static or a dynamic load. This software has the ability to generate Discrete Fracture Networks (DFNs) to build a fractured model. These DFNs are composed of multiple disk-shaped elements that represent each a fracture of a defined joint set. These disks have the properties of the fractures mapped in the field (Pierce 2017). These properties are mainly orientation, size and density, which can also be extracted from a laser scan extracted point cloud. This work presents the implementation and validation of a methodology combining laser scanning technology with Discrete Element Modeling as a tool for characterizing, preventing, and managing structurally controlled instability that may affect large-opening underground mines.

2 DESIGN AND ANALYSIS

The Laser scanning with DEM integration process consisted of five main stages: 1) Laser scanning, 2) Virtual Discontinuity Mapping (VDM), 3) DFN Generation, 4) Preliminary Discrete Element Modeling, and 5) Stochastic Modeling, which are described below.

The Laser scanning surveying campaign consisted of 9 laser scanner stations which were positioned approximately 13 m away from one another around the study area. The laser scanner operational conditions were set as 44.4 Million points per scan for the resolution and 1x for quality, which yielded an average point cloud density of 11 points/cm^2 and a scanning time of 5 minutes and 22 seconds per station. These stations were referenced and registered to each other, generating a final point cloud of the study area. The registration process yielded minimum overlap values of 25.2% and a mean point error of 4.3 mm. This final point cloud was used later for virtual discontinuity mapping (Monsalve et al. 2019).

The VDM process was performed by using the Maptek's point cloud processing software, I-Site Studio. This software contains a set of geotechnical analysis tools that can map discontinuities from a point cloud. When a fracture is observed on the point cloud a discontinuity element can be created by selecting the points belonging to the same discontinuity. This element contains information such as orientation, trace length and area of the mapped fracture. Such information can be used to characterize each discontinuity set. A total of 874 discontinuities were mapped in the study area. These were imported into Dips to identify the main discontinuity sets in the rock mass (Rocscience 2019). Once the main discontinuity sets were defined, these discontinuities were brought back to I-site where the spacing between fractures of each discontinuity set was measured. Figure 1 summarizes the VDM mapping and the statistical analysis for the trace length and the lineal fracture density of each identified structural set.

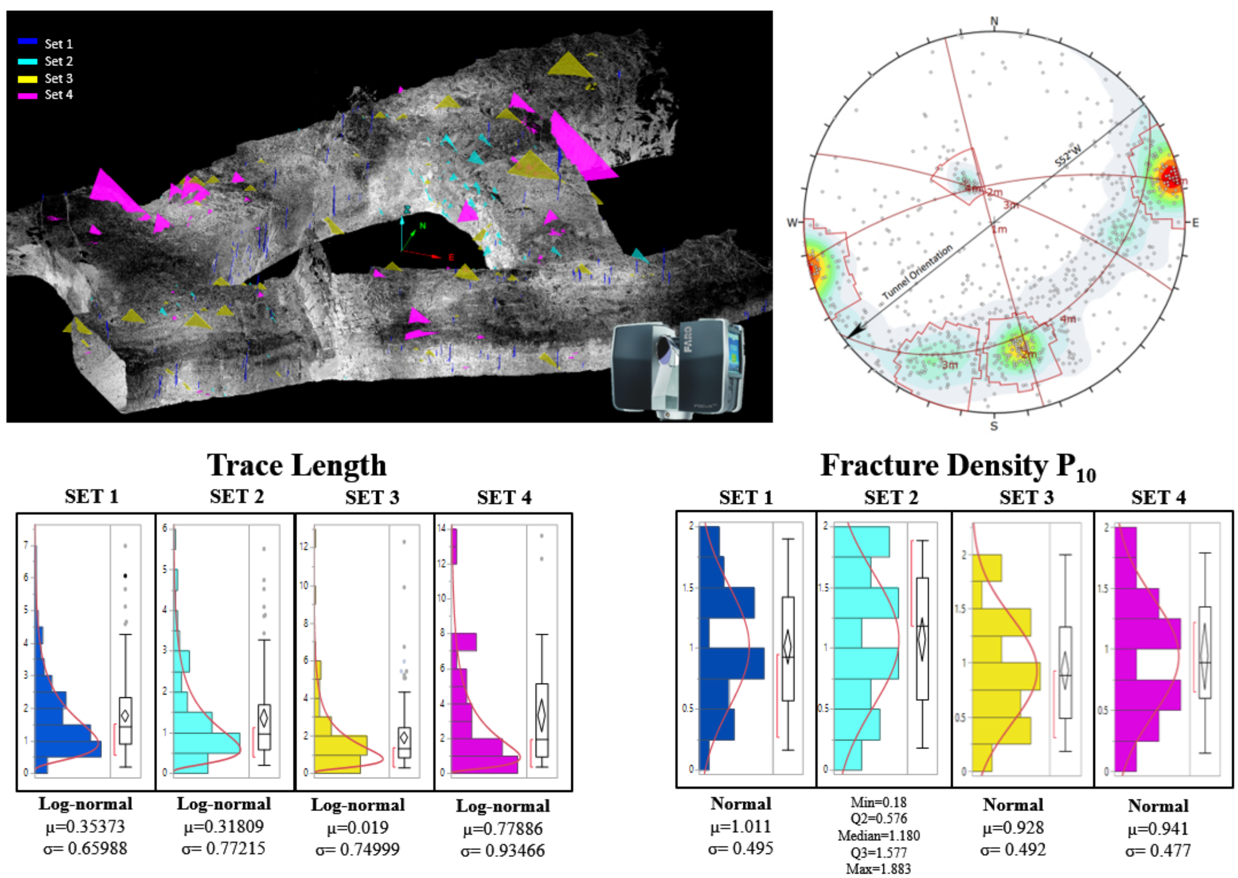

Figure 1. Virtual Discontinuity Mapping Summary.

Information obtained from the VDM was subsequently used to generate a Discrete Fracture Network for each discontinuity set. Table 1 summarizes the values used in *3DEC* to generate the fractured model. These DFNs were used to generate a fractured rock mass model by cutting the initial parent blocks. The cutting order was a relevant parameter to simulate the rock mass structure, since it significantly altered the fracturing model. For this study, the set corresponding to bedding planes were used to cut the model first, followed by Set 1 which corresponded to joints parallel to the dip of the body, followed by Sets 2 and 3 which corresponded to shear joints. Once the fractured rock mass model was built, the simulation took place. In this model a rigid block approach was assumed taking into account that the main failure mechanism observed in the field was gravity-induced block failure. The excavation of a 12.8 m wide and 7.6 m high top preparation drift was simulated, and the amount and volume of failed blocks were assessed.

Table 1. Summary of values used to generate the Discrete Fracture Networks.

SET / PARAMETERS		S1 N=157	S2 N=127	S3 N=97	S4 (Bedding) N=45
Orientation	Dip [°]	88	68	75	29
	Dip Direction [°]	255	348	21	144
	K (Fisher)	103.9	102.4	69.5	197.3
Size	Distribution	Log-normal	Log-normal	Log-normal	Normal
	Mean	0.353	0.318	0.018	9
	Standard deviation	0.659	0.772	0.749	1
Density	Input area of fractures per unit volume (P_{32})	0.1	0.4	0.4	0.5
	Measured number of fractures per meter (P_{10})	1.3	1.1	0.6	0.6

Finally, considering that the nature of the DFNs used to build the fracture rock mass model is stochastic, a stochastic modeling approach was used. The same model was run 30 times, reporting the same information for each iteration. This was done by generating a master file which ran the model several times and varying the random seed number to ensure every result was different. The iteration number was stored in the text file along with the block information (Monsalve et al. 2019). This enabled the performance of further analyses on the extracted information. The analyzed parameters were total volume of failed blocks and amount of failed blocks per iteration. In order to validate the models, the results were compared with the 3-dimensional point clouds obtained from the laser scans. Two dimensional sections from both models were extracted and compared.

3 RESULTS AND DISCUSSION

The results obtained from this methodology allowed us to estimate the probability of rock failure based on the geometry and weight of failed blocks formed by the intersection of discontinuities in the section of interest. In the models, failed blocks were defined as those blocks that had displaced more than 2 cm and presented velocities higher than 5×10^{-5} mm/s, indicating that the blocks were in movement. Figure 2a indicates in red the failed blocks, while grey indicates those blocks that have not yet failed. Velocity vectors also are marked, indicating blocks that are still displacing. Figure 2b & c present the probability density functions obtained from the stochastic analysis. These results indicate that considering the present structural condition in this section of the mine, there is 35% probability for a total volume of 10 m^3 of rock blocks to fall in 20 m of tunneling advance. Results obtained from this methodology offer engineers an accurate tool to estimate the mass of failed blocks in excavations under a structurally controlled failure mechanism.

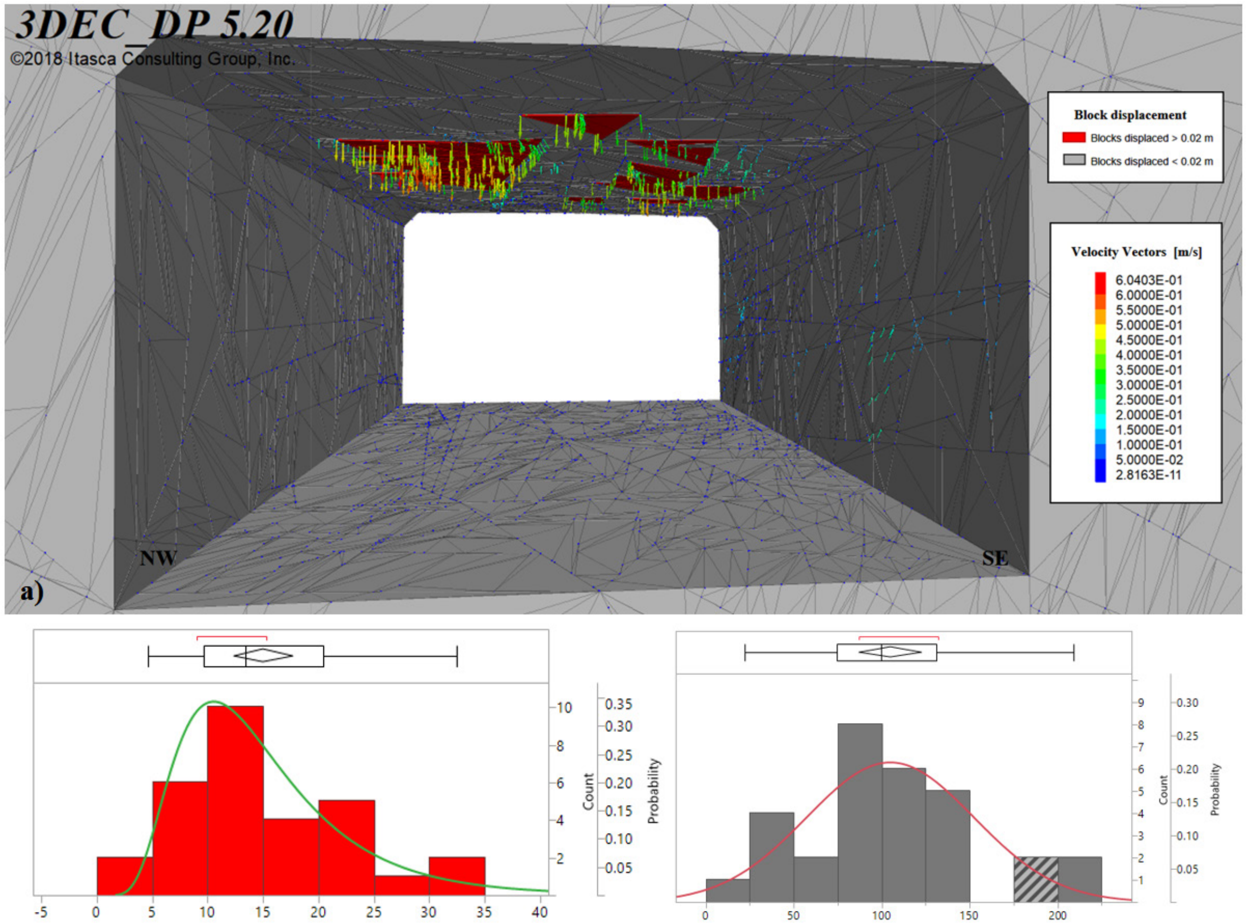

b)

Summary Statistics	
Distribution	Log-Normal
Mean	2.60
Standard Deviation	0.49

c)

Summary Statistics	
Distribution	Normal
Mean	104.87
Standard Deviation	47.58

Figure 2. a) Discrete element model indicating failed blocks, b) Probability density function for total volume of failed blocks, c) Probability density function for number of total failed blocks.

4 CONCLUSIONS

This methodology gives mining operators control measures to evaluate, map and mitigate risks associated with rock falls in underground mines, ultimately improving the safety in the underground limestone industry. This proposed methodology is based on a specific case study that does not meet the requirements to be designed with current industry empirically based guidelines. However, since it considers site-specific conditions, the general methodology proposed in this work can be applied to any mine experiencing similar failure mechanisms, ultimately ensuring workers safety in the underground stone mining industry.

REFERENCES

Brady, B. & Brown, E. 1985. *Rock Mechanics for Underground Mining.* UK: Chapman & Hall.

Esterhuizen, G.S., Dolinar, D.R., Ellenberg, J.L., & Prosser, L.J. 2011. *Pillar and Roof Span Design Guidelines for Underground Stone Mines.* Pittsburg: National Institute for Occupational Safety and Health.

Goodman, R. 1989. *Introduction to Rock Mechanics.* New York: Wiley.

Goodman, R. & Shi, G. 1985. *Block Theory and Its Application to Rock Engineering.* London: Prentice-Hall.

Itasca Consulting Group, Inc. 2016. *3DEC – 3 Dimensional Discrete Element Code, Ver. 5.2 User's Manual*. Itasca: Minneapolis.

Lorig, L. & Varona, P. 2013. Guidelines for numerical modelling of rock support for mines. *Ground Support 2013*, 81-105.

Monsalve, J., Baggett, J., Bishop, R. & Ripepi, N. 2018. A Preliminary Investigation for Characterization and Modeling of Structurally Controlled Underground Limestone Mines by Integrating Laser Scanning with Discrete Element Modeling. *North American Tunneling Conference.* Washington: SME.

Monsalve, J., Baggett, J., Bishop, R. & Ripepi, N. 2019. Application of Laser Scanning for Rock Mass Characterization and Discrete Fracture Network Generation in an Underground Limestone Mine. *International Journal of Mining Science and Technology*, 131-137.

Monsalve, J., Jon, B., Soni, A., Ripepi, N. & Hazzard, J. 2019. Stability Analysis of an Underground Limestone Mine Using Terrestrial Laser Scanning with Stochastic Discrete Element Modeling. *53rd US Rock Mechanics/Geomechanics ARMA Symposium.* New York: American Rock Mechanics Association.

Pierce, M. 2017. An Introduction to Random Disk Discrete Fracture Network (DFN) for Civil and Mining Engineering Applications. *ARMA e-Newslatter 20*, 3-8.

Rocscience. 2019. Rocscience. Retrieved from Dips online help: https://www.rocscience.com/help/dips/#t=dips%2FGetting_Started.htm. August 26, 2019.